

The effect of time-dependent infectiousness on epidemic dynamics

Nicholas W. Landry*

Department of Applied Mathematics, University of Colorado at Boulder, Boulder, Colorado 80309, USA

(Dated: June 1st, 2021)

In contrast to the common assumption in epidemic models that the rate of infection between individuals is constant, in reality, an individual's viral load determines their infectiousness. We compare the average and individual reproductive numbers, epidemic dynamics, and intervention strategies for a model incorporating time-dependent infectiousness and a standard SIR model for both fully-mixed and category-mixed populations. We find that the reproductive number only depends on the total infectious exposure and the largest eigenvalue of the mixing matrix and that these two effects are independent of each other. We also find that when we compare our time-dependent mean-field model to the SIR model with identical rates, the epidemic peak is advanced and more pronounced and modifying the infection rate function has a strong effect on the time dynamics of the epidemic. Lastly, we explore the effect of social and pharmaceutical interventions on our theoretical framework.

I. INTRODUCTION

Epidemic modeling has a rich tradition in network science [1–4] with standard models such as the SIS (Susceptible – Infected – Susceptible) and SIR (Susceptible – Infected – Removed) models, for which rigorous mathematical theory has been developed. There are also more complex spatio-temporal models that more accurately capture the dynamics of disease spread in the real world [5]. Much interest has been devoted to the accurate prediction of the spread of the SARS-CoV-2 pandemic [6, 7] and to answering questions such as the efficacy of different prevention measures and the risk factors of different social situations [8–10]. In traditional literature, the SIR model is a canonical example of modeling the spread of disease with total immunity. This model has common extensions such as the SEIR (Susceptible – Exposed – Infected – Recovered) when one wants to incorporate a latent period which captures delays between transmission and infectiousness. With most of these models, however, a key assumption is that an individual's infectivity is constant. However, we know that an individual's infectiousness varies over the duration of the infection, according to their viral load [11, 12]. We define a framework to extend the SIR model by dividing the single infectious compartment into n stages as has been considered by Ref. [13], known as the SI^KR model in Ref. [14], and assigning each stage a different infection rate as in Refs. [15, 16]. Other approaches have been considered, such as the message-passing approach [17, 18], mapping an individual's viral load to an infection probability [10], and looking at an infection density function [14, 19]. We use this approach to examine fully-mixed populations and theoretical networks constructed from category-based mixing, both static and temporal.

The structure of the paper is as follows. In Section II we describe a framework for modeling time-dependent

infectiousness. In Section III we use this model to create theoretical predictions for the reproductive number and we apply these predictions to several common cases. In Section IV we examine the effects of interventions in the form of vaccines and non-pharmaceutical interventions. Lastly, in Section V we discuss the implications of our theory.

II. MODEL

We propose a general mean-field model to describe the spread of an epidemic including time-dependent infectiousness. In the following, we will refer to this model as the viral load (VL) model.

We consider a population of N nodes. We assume that a node i 's intrinsic infectiousness is solely determined by the amount of time it has been infected, τ , and its corresponding viral load at that time, denoted $v_i(\tau)$, although other factors may be involved as well [8]. Several studies have examined the correspondence between an individual's viral load and their infectiousness [11, 12] but for this study, we simply define $\beta_i(\tau)$, the infectious rate function, as the rate at which node i transmits infection having been infected for a duration of time τ . Note that in the case where an infectious threshold exists [10, 20], we can express the function as $\beta_i(\tau)I_{\tau \in \delta}$, where $\delta = \{\tau \mid \beta_i(\tau) \geq c\}$ and c is the infectious threshold. This infectious rate function can vary in response to many factors such as asymptomatic versus symptomatic infection or severity of symptoms and be considered as being drawn according to some distribution. For the purposes of this study, however, we assume in our theoretical framework that while $\beta_i(\tau)$ is heterogeneous in time, that every member of the population has the same infectious rate function, i.e., $\beta_i(\tau) = \beta(\tau)$, $i = 1 \dots N$. We assume that nodes start in the susceptible compartment (S) and that an infected individual infected for time τ infects a susceptible node with rate $\beta(\tau)$. We approximate $\beta(\tau)$ by evaluating it at n discrete times $\tau_j = j\Delta\tau$, where $\Delta\tau$ is fixed and $n\Delta\tau = \tau_R$, the recovery time. Then

* nicholas.landry@colorado.edu

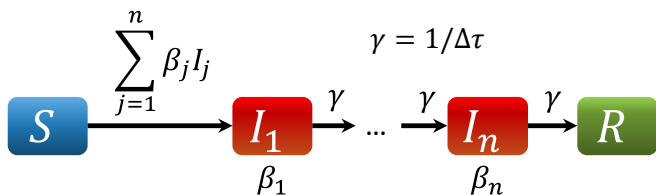


FIG. 1: An illustration of the VL model.

we divide the infectious compartment, I into n stages, I_j , $j = 1 \dots n$, each with an associated infection rate β_j , in a similar manner to Refs. [13, 16]. Lastly, nodes that transition through all infection states accumulate in the recovered (R) compartment.

We assume that the flow of infected individual between subsequent infectious compartments is deterministic and that upon entering the first infectious stage, an individual passes through all the subsequent stages as shown in Figure 1, meaning that $\gamma_i = 1/\Delta\tau$ where $\Delta\tau = \tau_R/n$.

III. DERIVATION OF THE POPULATION REPRODUCTIVE NUMBER

We derive the reproductive number for the viral load model described above that has been cast as a system of mean-field ODEs. First, we derive the reproductive number for a fully-mixed model and second, we derive the reproductive number for an arbitrary category-mixed population. We comment on the continuum limit for both cases and derive specific closed-form solutions for the reproductive number for a configuration model static network, and an activity model temporal network.

A. Fully-mixed population

Consider a fully-mixed population of N individuals and an infectious rate function, $\beta(\tau)$. In our formalism, we denote the fraction of the population in the susceptible, j th infectious stage, and the recovered stage as S , I_j , $j = 1 \dots n$, and R respectively and note that $S + \sum_{j=1}^n I_j + R = 1$ by conservation. Assuming that an individual's infection status is independent of the infection status of its neighbors, as done in Ref. [16], we can write the following system of mean-field equations as

$$\frac{dS}{dt} = -S \sum_{j=1}^n \beta_j I_j, \quad (1a)$$

$$\frac{dI_1}{dt} = -\frac{I_1}{\Delta\tau} + S \sum_{j=1}^n \beta_j I_j, \quad (1b)$$

$$\frac{dI_j}{dt} = \frac{I_{j-1} - I_j}{\Delta\tau}, \quad j = 2 \dots n, \quad (1c)$$

$$\frac{dR}{dt} = \frac{I_n}{\Delta\tau}. \quad (1d)$$

By construction, an infected node will always transition through all the infectious states until it reaches the recovered state. However, we are not interested in whether infected nodes transition through all the states, but rather whether susceptible nodes become infected. In Ref. [21], the authors introduce the notion of a *next generation matrix* (NGM) which decomposes the linearized system into infectious transmissions, T , and non-infectious transitions, Σ , where transmissions move susceptible nodes to infected compartments and transitions move infected nodes to other infectious states. As done in Ref. [21], we exclude the susceptible and recovered states. The linearized system can be written as

$$\mathbf{I}' = \frac{1}{\Delta\tau} \begin{pmatrix} -1 + \beta_1 \Delta\tau & \beta_2 \Delta\tau & \dots & \dots & \beta_n \Delta\tau \\ 1 & -1 & 0 & \dots & 0 \\ 0 & 1 & -1 & \ddots & \vdots \\ \vdots & \ddots & \ddots & \ddots & 0 \\ 0 & \dots & 0 & 1 & -1 \end{pmatrix} \mathbf{I},$$

where $\mathbf{I} = (I_1, \dots, I_n)^T$. We split the matrix into transmissions and transitions and according to Ref. [21], the reproductive number R_0 is given by $\rho(-T\Sigma^{-1})$ which for the fully mixed case evaluates to

$$R_0 = \sum_{i=1}^n \beta_i \Delta\tau, \quad (2)$$

which matches the value found in Ref. [16].

This result indicates that any infectious rate function that has the same total infectiousness or *exposure* yields the same reproductive number, regardless of the particular function. This, however, does not hold for the time scale on which the epidemic spreads as we will see later.

B. Discrete category-mixed population

Now we consider a population with N individuals each of which belong to a category c_i , $i = 1 \dots n_c$. These mixing categories can encode many different characteristics such as degree-based mixing [22], age-mixing [23], spatial meta-population mixing [5], mixing due to travel and many other types of mixing.

We denote the probability that sub-populations c_i and c_j interact with each other as $p(c_i, c_j)$ and the probability that a node belongs to category i as $p(c_i)$. We discretize the infectious states not only by the progression of the infection, but by the category to which that individual belongs as well. This model has $(n+2)n_c$ states: n_c susceptible states, $S^{c_1}, \dots, S^{c_{n_c}}$; nn_c susceptible states, $I_1^{c_1}, \dots, I_1^{c_{n_c}}, \dots, I_n^{c_1}, \dots, I_n^{c_{n_c}}$; and n_c recovered states, R^1, \dots, R^{n_c} . Then the mean-field model becomes for

each category c

$$\frac{dS^c}{dt} = -S^c \sum_{i=1}^{n_c} \sum_{j=1}^n p(c, c_i) p(c_i) \beta_j I_j^{c_i}, \quad (3a)$$

$$\frac{dI_1^c}{dt} = -\frac{I_1^c}{\Delta\tau} + S^c \sum_{i=1}^{n_c} \sum_{j=1}^n p(c, c_i) p(c_i) \beta_j I_j^{c_i}, \quad (3b)$$

$$\frac{dI_j^c}{dt} = \frac{I_{j-1}^c - I_j^c}{\Delta\tau}, \quad j = 2 \dots n, \quad (3c)$$

$$\frac{dR^c}{dt} = \frac{I_n^c}{\Delta\tau}. \quad (3d)$$

The linearized ODE is the following block-matrix system of equations:

$$\mathbf{I}' = \frac{1}{\Delta\tau} \begin{pmatrix} -I + \beta_1 \Delta\tau P & \beta_2 \Delta\tau P & \dots & \dots & \beta_n \Delta\tau P \\ I & -I & 0 & \dots & 0 \\ 0 & I & -I & \ddots & \vdots \\ \vdots & \ddots & \ddots & \ddots & 0 \\ 0 & \dots & 0 & I & -I\tau \end{pmatrix} \mathbf{I},$$

where

$$P = \begin{pmatrix} p(c_1, c_1) p(c_1) & \dots & p(c_1, c_{n_c}) p(c_{n_c}) \\ \vdots & \ddots & \vdots \\ p(c_{n_c}, c_1) p(c_1) & \dots & \beta_i p(c_{n_c}, c_{n_c}) p(c_{n_c}) \end{pmatrix},$$

$\mathbf{I} = (I_1^{c_1}, \dots, I_1^{c_{n_c}}, \dots, I_n^{c_1}, \dots, I_n^{c_{n_c}})^T$, and I is the identity matrix.

Splitting the matrix into transmissions and transitions, the next-generation matrix is

$$-T\Sigma^{-1} = \begin{pmatrix} P \sum_{i=1}^n \beta_i \Delta\tau & P \sum_{i=2}^n \beta_i \Delta\tau & \dots & P \beta_n \Delta\tau \\ 0 & \dots & \dots & 0 \\ \vdots & \ddots & \ddots & \vdots \\ 0 & \dots & \dots & 0 \end{pmatrix}. \quad (4)$$

Then, the reproductive number evaluates to

$$R_0 = \rho(P) \sum_{i=1}^n \beta_i \Delta\tau, \quad (5)$$

which indicates that the epidemic threshold depends both on the infectious exposure and the matrix of mixing probabilities and that these two quantities are independent.

C. The continuum limit

For each case described prior, it is natural to want to take the limit as the number of infectious compartments approaches infinity and $\Delta\tau \rightarrow 0$. For the fully-mixed case, the reproductive number becomes

$$R_0 = \int_0^{\tau_R} \beta(\tau) d\tau, \quad (6)$$

and similarly, for category-based mixing, it is

$$R_0 = \rho(P) \int_0^{\tau_R} \beta(\tau) d\tau. \quad (7)$$

Alternatively, we can treat τ as a continuous quantity and track the infectiousness, $I(t, \tau)$, as a function of the overall time and how long an individual has been infected. When τ is continuous, $\Delta\tau \rightarrow 0$ and the finite difference $(I_{j-1} - I_j)/\Delta\tau$ in Eqns. (1c) and (3c) becomes a derivative with respect to τ . With these assumptions, our ODE model can be expressed as the transport equation with boundary conditions handling the infection and recovery. For the fully-mixed case, this is

$$\frac{\partial I(t, \tau)}{\partial t} = -\frac{\partial I(t, \tau)}{\partial \tau}, \quad (8a)$$

$$I(t, 0) = S \int_0^{\tau_R} \beta(\tau) I(t, \tau) d\tau, \quad (8b)$$

$$S = 1 - \int_0^{\tau_R} I(t, \tau) d\tau - \int_0^t \frac{\partial I(t, \tau)}{\partial \tau} \Big|_{\tau=\tau_R} dt, \quad (8c)$$

$$I(t, \tau_R) = 0. \quad (8d)$$

This perspective lends physical interpretation to our model; an infected individual is transported through the infectious stages and the boundaries merely introduce new individuals into this transport process and remove recovered individuals at the other boundary.

D. Examples

In the following, we apply our category-mixing framework to two cases, a static degree-based configuration model and a temporal activity-based model.

1. Configuration model

Consider a network of size N with a degree sequence $\mathbf{k} = (k_1, \dots, k_N)^T$ and nodes connected by links at random, which specifies the configuration model, described more in Ref. [24]. For the standard SIR model on a configuration model network, the reproductive number is $R_0 = \beta \langle k^2 \rangle / (\gamma \langle k \rangle)$ [1]. We assume that a node's degree completely specifies its dynamic behavior, which ignores effects from a node's other characteristics. From the degree sequence \mathbf{k} , we can compute the discrete probability distribution $p(k) = N(k)/N$, where $N(k)$ is the number of nodes in the degree sequence that have degree k , and the list of unique degrees in the degree sequence, \mathbf{k}_u . Lastly, we define the m -th moment of a quantity q as $\langle q^m \rangle = \sum_{i=1}^N q_i^m / N$. From our general formalism in Section III B, the degree mixing matrix is

$$P = \frac{1}{\langle k \rangle} (\mathbf{k}_u \mathbf{p})^T \mathbf{k}_u. \quad (9)$$

where $\mathbf{k}_u \mathbf{p} = (k_1 p(1), \dots, k_{max} p(k_{max}))^T$ and $\mathbf{k}_u = (k_1, \dots, k_{max})^T$. The largest eigenvalue of this matrix is $\langle k^2 \rangle / \langle k \rangle$ and so the reproductive number is

$$R_0 = \frac{\langle k^2 \rangle}{\langle k \rangle} \int_0^{\tau_R} \beta(\tau) d\tau. \quad (10)$$

Setting $\gamma = 1/\tau_R$ and $\beta = \overline{\beta(\tau)} = \int_0^{\tau_R} \beta(\tau) d\tau / \tau_R$ for the SIR model yields the reproductive numbers derived in Ref. [1].

2. Activity model

Our category-based framework applies not only to static contact structures, but to temporal networks as well. We consider the *activity model* first presented in Ref. [25]. Given a temporal network of size N , suppose that each node i has an *activity rate* a_i , which denotes the probability per unit time that the node is active. At each discrete time, each node is either active or idle, and each active node forms m connections with other nodes, active or inactive. Unlike degrees which are discrete for an unweighted network, these activity rates are continuous, and to use our category-based mixing framework, we assume that we can bin these rates into discrete categories, $a_i, i = 1 \dots n_a$ and later take the continuum limit as before. We denote the probability that a node has an activity rate a_i as $p(a_i)$. Then the probability that nodes with activity rates a_i and a_j are connected at any given time is $(a_i + a_j) \frac{m}{N}$ and the time-averaged mixing matrix is

$$P_{ij} = \frac{m(a_i + a_j)}{N} p(a_j),$$

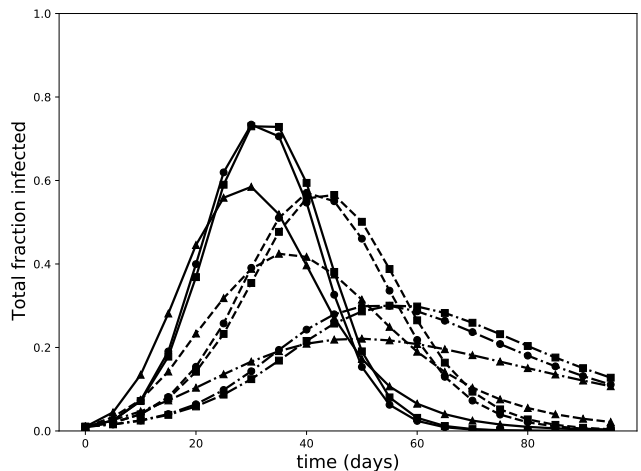
which can be written $P = \mathbf{1b}^T + \mathbf{c}\mathbf{p}^T$ where $\mathbf{b} = (m a_1 p(a_1), \dots, m a_{n_a} p(a_{n_a}))^T$, $\mathbf{c} = (m a_1, \dots, m a_{n_a})^T$, and $\mathbf{p} = (p(a_1), \dots, p(a_{n_a}))^T$. Observing that this is a rank-2 matrix, the analytical solution for the Perron-Frobenius eigenvalue is $(m\langle a \rangle + m\sqrt{\langle a^2 \rangle})$ and

$$R_0 = (m\langle a \rangle + m\sqrt{\langle a^2 \rangle}) \int_0^{\tau_R} \beta(\tau) d\tau. \quad (11)$$

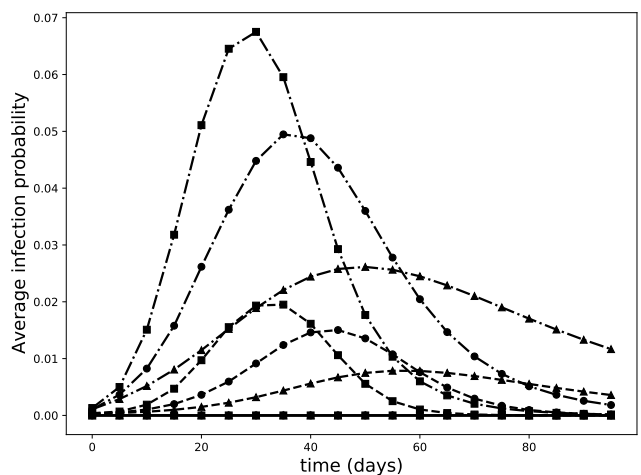
In Ref. [25], they derive the epidemic threshold for the activity model as $\beta_c/\gamma = 2\langle a \rangle / (\langle a \rangle + \sqrt{\langle a^2 \rangle})$. As before, setting $\gamma = 1/\tau_R$ and $\beta = \overline{\beta(\tau)}$ yields the same result.

E. Comparing mean-field time dynamics

We compare the time dynamics of the SIR model with that of the VL model with different infectious rate functions. For the following figures, we fix $N = 10^4$, $R_0 = 3$, $\tau_R = 21$ days, $\arg \max_{\tau} \beta(\tau) = 4$ days, no transmission below 20% of the maximum infectious rate, and 100 infectious compartments. For the degree-mixed cases, we used



(a) Infected fraction over time



(b) Average infection probability over time

FIG. 2: Time response of the infected fraction and average infection probability per individual for different contact structure and epidemic model. In both figures, the solid, dashed, and dot-dashed lines indicate the fully-mixed, uniform degree distribution, and power-law degree distribution cases respectively. Likewise, the square, circle, and triangle symbols indicate the VL model with $\beta(\tau) \propto \tau \exp(\tau/4)$, the VL model with $\beta(\tau) = c$, and the SIR model respectively.

a uniform degree distribution on [10, 30] and a power-law degree distribution $p(k) \propto k^{-3}$ on [10, 1000] such that both had an expected mean degree of 20. In this work, we consider a constant-valued infectious rate function as a null model and a scaled gamma distribution as in Ref. [12].

From Figure 2a we see that the VL models have more significant epidemic peaks due to the deterministic flow through infectious compartments and the peak of the SIR model is delayed relative to both VL models. It is interesting to note that the VL models fundamentally change

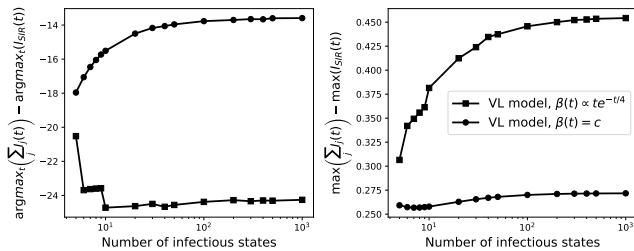


FIG. 3: Comparing the difference in the infected peak magnitude and infected peak time for the VL model and the SIR model.

the time scale of the epidemic when compared to the SIR model and that the effect of the particular model on the time dynamics is larger than the effect of heterogeneity in the contact structure. Not all infectious compartments are created equal, however; someone at their peak infectiousness contributes much more to the spread of an epidemic than someone who has almost recovered or just gotten infected. If we observe the mean infection probability per individual over time, where each compartment is scaled by its intrinsic infectivity, we see that the heterogeneity of the contact structure plays a much larger role as seen in Figure 2b.

With the approach that we take of discretizing the infectious compartments, we perform numerical experiments to analyze the number of states at which we can expect the model to reasonably approximate the continuous dynamics. For a small number of states, the discretized values of the infectious rate function fluctuate leading to the non-monotone and non-smooth trends we see in Figure 3 for the infectious rate function proportional to a gamma distribution. As the number of infectious states is increased, the epidemic dynamics converge to that of the VL model with a continuous infectious rate function. From Figure 3, approximately 100 infectious states are necessary to accurately capture key features of the epidemic response.

IV. INTERVENTIONS

We use the VL model framework to discuss the effect of interventions, both pharmaceutical and social. We examine the effect of vaccines which attenuate, but do not eliminate, transmission, as well as the effect of a detectability limit corresponding to a person’s infectiousness.

A. Vaccines

Suppose that a fraction of the population ρ is vaccinated and that vaccination prevents an individual from getting severely ill but does not prevent transmission [26], rather modifying the infectious rate function to be $\beta_v(t)$,

where $\|\beta_v(\tau)\|_1 \ll \|\beta(\tau)\|_1$. If we instead think of vaccinated individuals being 100% transmission-blocking, this is akin to setting $\beta_v(\tau) = 0$, which effectively removes those individuals from the population. Following the same steps as above, the reproductive number for random vaccination becomes the weighted average of the vaccinated and non-vaccinated exposure, written

$$R_0 = \int_0^{\tau_R} [(1 - \rho)\beta(\tau) + \rho\beta_v(\tau)] d\tau \quad (12)$$

for a fully-mixed population and similarly, for category-based mixing,

$$R_0 = \rho(P) \int_0^{\tau_R} [(1 - \rho)\beta(\tau) + \rho\beta_v(\tau)] d\tau. \quad (13)$$

There are many different vaccination strategies that we do not consider here, but refer the reader to Refs. [27, 28] for more discussion.

B. Social interventions

In complement to immunity-related interventions, we also explore the effect of detectability. Suppose that above a certain detectability threshold β_D an individual will test positive or notice that they are ill and that this corresponding detection time is $\tau_D \ll \tau_R$. If this individual is socially responsible and quarantines or limits their contact with others, this has the effect of “cutting the tail” of the infectious rate function meaning that an individual’s total viral exposure is $\int_0^{\tau_D} \beta(\tau) d\tau \ll \int_0^{\tau_R} \beta(\tau) d\tau$ which has the effect of lowering the expected number of secondary infections by a factor of $\int_0^{\tau_R} \beta(\tau) d\tau / \int_0^{\tau_D} \beta(\tau) d\tau$ for every individual who isolates upon detection.

V. DISCUSSION

In our analysis, we see that time-dependent infectiousness causes a fundamental change in the time dynamics, and perspective on intervention strategies despite an epidemic threshold matching classical theory. Our result that contact structure and the infectiousness have independent effects on the reproductive number. Accounting for time-dependent infectiousness doesn’t affect predictions on whether an epidemic will grow or die out, but it has strong implications on the time scale and prevalence of the resulting dynamics. In this work, we did not explore the effect of individual variation in the infectious rate function on the time dynamics, though we comment that the reproductive number will simply be the integral of the average of these functions with respect to their distribution. Our model can be written as the transport equation PDE in the continuum limit which validates our observations that an epidemic is akin to a traveling wave through the infectious stages.

In this study, we have only considered the population reproductive number, though it is well known that merely studying the population reproductive number without examining the heterogeneity in the number of secondary infections leaves out key information [8]. Superspreading events are the result of this stochasticity and can often be responsible for the transmission of an epidemic. One could use our framework to frame the distribution of secondary infections as a combination of the effects of contact-based and infectiousness-based heterogeneity.

ACKNOWLEDGEMENTS

I would like to thank Ren Stengel, Daniel Larremore, Juan G. Restrepo, and Subekshya Bidari for many helpful conversations and insights.

DATA AVAILABILITY

All code used in this study can be found at <https://github.com/nwlandry/time-dependent-infectiousness>.

-
- [1] M. Boguñá and R. Pastor-Satorras, Epidemic spreading in correlated complex networks, *Physical Review E* **66**, 047104 (2002).
- [2] R. Pastor-Satorras and A. Vespignani, Epidemic dynamics in finite size scale-free networks, *Physical Review E* **65**, 035108 (2002).
- [3] M. E. J. Newman, Spread of epidemic disease on networks, *Physical Review E* **66**, 016128 (2002).
- [4] R. Pastor-Satorras, C. Castellano, P. Van Mieghem, and A. Vespignani, Epidemic processes in complex networks, *Reviews of Modern Physics* **87**, 925 (2015).
- [5] D. Balcan, B. Gonçalves, H. Hu, J. J. Ramasco, V. Colizza, and A. Vespignani, Modeling the spatial spread of infectious diseases: The GLObal Epidemic and Mobility computational model, *Journal of Computational Science* **1**, 132 (2010).
- [6] A. Arenas, W. Cota, J. Gómez-Gardeñes, S. Gómez, C. Granell, J. T. Matamalas, D. Soriano-Paños, and B. Steinegger, Modeling the Spatiotemporal Epidemic Spreading of COVID-19 and the Impact of Mobility and Social Distancing Interventions, *Physical Review X* **10**, 041055 (2020).
- [7] B. Banerjee, P. K. Pandey, and B. Adhikari, A model for the spread of an epidemic from local to global: A case study of COVID-19 in India, arXiv:2006.06404 [physics, q-bio] (2020), arXiv:2006.06404 [physics, q-bio].
- [8] B. M. Althouse, E. A. Wenger, J. C. Miller, S. V. Scarpino, A. Allard, L. Hébert-Dufresne, and H. Hu, Superspreading events in the transmission dynamics of SARS-CoV-2: Opportunities for interventions and control, *PLOS Biology* **18**, e3000897 (2020).
- [9] G. St-Onge, V. Thibeault, A. Allard, L. J. Dubé, and L. Hébert-Dufresne, Social confinement and mesoscopic localization of epidemics on networks, *Physical Review Letters* **126**, 098301 (2021), arXiv:2003.05924.
- [10] D. B. Larremore, B. Wilder, E. Lester, S. Shehata, J. M. Burke, J. A. Hay, M. Tambe, M. J. Mina, and R. Parker, Test sensitivity is secondary to frequency and turnaround time for COVID-19 surveillance, medRxiv , 2020.06.22.20136309 (2020).
- [11] M. Marks, P. Millat-Martinez, D. Ouchi, C. h Roberts, A. Alemany, M. Corbacho-Monné, M. Ubals, A. Tobias, C. Tebé, E. Ballana, Q. Bassat, B. Baro, M. Vall-Mayans, C. G-Beiras, N. Prat, J. Ara, B. Clotet, and O. Mitjà, Transmission of COVID-19 in 282 clusters in Catalonia, Spain: A cohort study, *The Lancet Infectious Diseases* **21**, 629 (2021).
- [12] X. He, E. H. Y. Lau, P. Wu, X. Deng, J. Wang, X. Hao, Y. C. Lau, J. Y. Wong, Y. Guan, X. Tan, X. Mo, Y. Chen, B. Liao, W. Chen, F. Hu, Q. Zhang, M. Zhong, Y. Wu, L. Zhao, F. Zhang, B. J. Cowling, F. Li, and G. M. Leung, Temporal dynamics in viral shedding and transmissibility of COVID-19, *Nature Medicine* **26**, 672 (2020).
- [13] A. L. Lloyd, Realistic Distributions of Infectious Periods in Epidemic Models: Changing Patterns of Persistence and Dynamics, *Theoretical Population Biology* **60**, 59 (2001).
- [14] I. Z. Kiss, J. Miller, and P. L. Simon, *Mathematics of Epidemics on Networks: From Exact to Approximate Models*, Interdisciplinary Applied Mathematics (Springer International Publishing, 2017).
- [15] J. Ma and D. J. D. Earn, Generality of the Final Size Formula for an Epidemic of a Newly Invading Infectious Disease, *Bulletin of Mathematical Biology* **68**, 679 (2006).
- [16] J. M. Hyman, J. Li, and E. Ann Stanley, The differential infectivity and staged progression models for the transmission of HIV, *Mathematical Biosciences* **155**, 77 (1999).
- [17] B. Karrer and M. E. J. Newman, Message passing approach for general epidemic models, *Physical Review E* **82**, 016101 (2010).
- [18] N. Sherborne, J. C. Miller, K. B. Blyuss, and I. Z. Kiss, Mean-field models for non-Markovian epidemics on networks, *Journal of Mathematical Biology* **76**, 755 (2018).
- [19] G. Röst, Z. Vizi, and I. Z. Kiss, Pairwise approximation for SIR-type network epidemics with non-Markovian recovery, *Proceedings of the Royal Society A: Mathematical, Physical and Engineering Sciences* **474**, 20170695 (2018).
- [20] M. J. Mina, R. Parker, and D. B. Larremore, Rethinking Covid-19 Test Sensitivity — A Strategy for Containment, *New England Journal of Medicine* **383**, e120 (2020).
- [21] O. Diekmann, J. a. P. Heesterbeek, and M. G. Roberts, The construction of next-generation matrices for compartmental epidemic models, *Journal of The Royal Society Interface* **7**, 873 (2010).
- [22] J. C. Miller, A. C. Slim, and E. M. Volz, Edge-based compartmental modelling for infectious disease spread, *Journal of The Royal Society Interface* **9**, 890 (2012).
- [23] D. Mistry, M. Litvinova, A. Pastore y Piontti, M. Chinazzi, L. Fumanelli, M. F. C. Gomes, S. A. Haque, Q.-H. Liu, K. Mu, X. Xiong, M. E. Halloran, I. M. Longini,

- S. Merler, M. Ajelli, and A. Vespignani, Inferring high-resolution human mixing patterns for disease modeling, *Nature Communications* **12**, 323 (2021).
- [24] B. K. Fosdick, D. B. Larremore, J. Nishimura, and J. Ugander, Configuring Random Graph Models with Fixed Degree Sequences, *SIAM Review* **60**, 315 (2018).
- [25] N. Perra, B. Gonçalves, R. Pastor-Satorras, and A. Vespignani, Activity driven modeling of time varying networks, *Scientific Reports* **2**, 469 (2012).
- [26] M. Lipsitch and R. Kahn, Interpreting vaccine efficacy trial results for infection and transmission, *Vaccine* 10.1016/j.vaccine.2021.06.011 (2021).
- [27] P. Holme, Efficient local strategies for vaccination and network attack, *EPL (Europhysics Letters)* **68**, 908 (2004).
- [28] J. C. Miller and J. M. Hyman, Effective vaccination strategies for realistic social networks, *Physica A: Statistical Mechanics and its Applications Disorder and Complexity*, **386**, 780 (2007).